Scientific Journal of Impact Factor (SJIF): 5.71

e-ISSN (O): 2348-4470
p-ISSN (P): 2348-6406

International Journal of Advance Engineering and Research Development

International Conference on Momentous Role of Nanomaterials in Renewable Energy Devices

Volume 5, Special Issue 07, April-2018 (UGC Approved)

INFLUENCE OF SULFUR SOURCES AND SOLVENTS ON THE OPTICAL, STRUCTURAL AND MORPHOLOGICAL PROPERTIES OF $CuInS_2$ NANOCRYSTALS BY HOT-INJECTION METHOD

C. Neela Mohan and V. Renuga[#]

Department of Chemistry, National College (Autonomous), Tiruchirappalli-01, Tamilnadu, India.

Abstract - *Non-toxic $CuInS_2$ nanocrystals as the visible-near infrared light emitting materials has attracted a considerable attention in a various technological fields such as LED, bioimaging, etc., In this investigation, $CuInS_2$ nanocrystals were successfully synthesized through hot-injection technique employing reactions of copper (II) acetate and indium (III) chloride with sulfur powder (S-OLA) or dodecanethiol (DDT) as a source of sulfur. Here, the reaction was carried out using two different solvents medium, such as diphenylether (DPE) as a coordinating solvent and 1-octadecene (ODE) as a non-coordinating solvent. Oleylamine (OLA) a capping agent is the only interacting with the starting precursor materials (Cu^+ and In^{3+}). The precursors play a major role on the seed formation and growth of the nanocrystals. Conversely, the solvents and sulfur source influence morphology and size of the resulting nanocrystals. The morphology of the synthesized nanocrystals were in cubic ZB form when ODE as a solvent and hexagonal WZ structure when diphenyl ether plays as solvent. The synthesized $CuInS_2$ nanocrystals were characterized by ultraviolet visible (UV-Vis), photoluminescence (PL), cyclic voltammetry (CV), X-ray diffraction (XRD) and high resolution transmission electron microscopy (HR-TEM).*

Keywords: *$CuInS_2$ Nanocrystals, Hot-injection Method, Semiconductors, Solvent effect, cyclic voltammetry (CV) and Morphology.*

I. INTRODUCTION

Recently, I-III-VI_2 ternary semiconductor compounds exist with direct bandgap of about 1.5 eV have excellent properties like low toxicity, high absorption coefficient and high theoretical photovoltaic conversion efficiency (about 25% to 30%) at room temperature[1-3]. Colloidal $CuInS_2$ nanoparticles, or $CuInS_2$ ink, are best known among the ternary I–III–VI_2 semiconductors and usually applied in photovoltaics [4], optics [5], electronic [6] and bioimaging [7]. The high absorption coefficient ($10^5 cm^{-1}$), tuneable electrical conductivity (n-type or p-type), excellent direct band gap (1.5 eV) and environmentally friendly nature makes $CuInS_2$ as an ideal candidate to be used as a p-type light absorbing materials in the ink jet printing solar cells [8-10]. According to previous studies, $CuInS_2$ nanocrystals exist in three different crystal structures: chalcopyrite, zinc blende, and wurtzite [11-13]. Chalcopyrite $CuInS_2$ is the most common existing phase at room temperature, whereas those with zinc blende and wurtzite structures are stable only at high temperatures.

Several groups have tried to modify the process for better shape control with improved crystallinity using different solvent and sulfur source for the synthesis of $CuInS_2$ [14-17]. Hepp and co-workers have synthesized $CuInSe_2$ nanocrystals using molecular single source precursors [18]. Hwang and co-workers have suggested a microwave enhanced solvothermal method and they showed diverse nanostructured morphologies of $CuInSe_2$ [19]. The Korgel group have demonstrated uniform-sized trigonal pyramidal $CuInSe_2$ nanocrystalss by using selenourea as a Se precursor [20]. Qian and co-workers demonstrated $CuInSe_2$ nanocrystals prepared in the autoclave by employing an alkylamine as a solvent [21,22]. Malik*et al* synthesized tri-n-octylphosphine oxide (TOPO)-capped cubic $CuInSe_2$ nanocrystals following the conventional procedure of quantum dot synthesis [23]. Very recently, Kruszynska et al reported shape-controlled synthesis of wz-$CuInS_2$ nanocrystals by methods of colloidal chemistry using the combination of two solvents and different sulfur sources [24].

Based on the literature survey, we have synthesized zinc blende and wurtzite nanocrystals of $CuInS_2$ using two different solvents (Octadecene and Diphenyl ether) and sulfur source (DDT and Sulfur powder). By controlling the reaction parameters, the $CuInS_2$ nanocrystals with spherical and hexagonal-like shapes were obtained. The obtained $CuInS_2$ nanocrystals were studied by UV–Vis absorption spectroscopy, PL spectroscopy (PL), cyclic voltammetry (CV), and powder X-ray diffraction (XRD, transmission electron microscopy (TEM) and energy dispersive X-ray analysis (EDX) The prepared nanocrystals exhibited high stability in an organic solvent.

II. EXPERIMENTAL METHODS

A. Materials

Copper (II) acetate ($Cu(OAc)_2$, 98%) and 'S'(sulfur 99.99%) were purchased from Alfa Aesar. Indium (III) chloride ($InCl_3$), Oleylamine (OLA, C-18 content 80%-90%), Diphenylether (DPE), 1-dodecanethiol (DDT) were purchased from Aldrich and used as such without further purifications.

B. Synthesis of $CuInS_2$ nanocrystals

The $CuInS_2$ nanocrystals were synthesized by hot injection technique using modified literature procedure [24], in which $Cu(OAc)_2$. $2H_2O$ and $InCl_3$ serve as the Cu^+ and In^{3+} sources, sulfur powder and DDT as 'S' source. Diphenylether (coordinating) and octadecene (non-coordinating) serves as the solvent and oleylamine as a stabilizer.

C. Techniques

In this technique, $Cu(OAc)_2$ (0.1 mmol), $InCl_3$ (0.1 mmol) were mixed with 5 mL of oleylamine and 10 mL diphenylether or 10 mL ODE in a 50 ml three necked flask. The mixture was heated to 100^{o}C under vacuum and stirred for at least 30 min till precursors were start to dissolve. Next the solution temperature was increased to 150^{o}C under N_2 condition until a clear solution was obtained. After that, the sulfur stock [0.4 mmol of sulfur dissolved in 2 mL oleylamine or 2 mL of DDT in oleylamine] solution was injected into reaction solution. Then the temperature was increased to 230^{o}C and maintained the same temperature for 30 min. The heating source was removed and the solution was cooled down to room temperature. $CuInS_2$ nanocrystals were collected by adding 30 ml of ethanol until the solution turned into turbid and precipitating by centrifugation (4000rpm, 10min). The collected nanoparticles were purified more than two times again with chloroform /ethanol co-solvent by centrifugation. The formed $CuInS_2$ nanocrystals were finally dried at 80^{o}C for 5 hours at oven.

D. Characterization

UV-Vis spectra of synthesized $CuInS_2$ nanocrystals were recorded using a Perkins–Elmer Lambda 35 UV–Vis spectrophotometer. The emission spectra of the prepared samples were obtained on fluorescence spectrophotometer. The crystalline structure of synthesized $CuInS_2$ nanocrystals was studied by X-ray diffraction (XRD) technique. The X-ray diffraction studies were carried out using XRD X'PERT-PRO diffractometer in the range of 20-60^o using CuKα radiation of wavelength λ=1.5406Å. The surface morphology and elemental composition of the nanocrystals were investigated by Transmission electron microscopy (TEM) and Energy Dispersive X-ray Spectroscopy (EDX).

III. RESULTS AND DISCUSSION

A. Absorption spectra

The UV-Vis spectra of oleylamine capped $CuInS_2$ nanocrystals using two different solvent (coordinating and non-coordinating) and two different sulfur sources investigated in the range of 300-1100 nm were recorded and depicted in Figure 1. The UV-Vis adsorption spectra of nanocrystals prepared at different conditions showed multiple onset absorption peaks with various shape and sizes of the prepared nanocrystals. The Figure.1 depicts the absence of obvious absorption peak present in the system.

Using ODE as a solvent and sulfur powder as sulfur source, we found the onset adsorption peak at 674 nm whereas ODE as solvent and DDT as sulfur source, the onset adsorption falls down from 674 to 653 nm, which has significantly blue-shifted from that of bulk $CuInS_2$ (810 nm) and is consistent with the expected quantum confinement effect.

In another case, we use DPE as a solvent and DDT and sulfur powder as sulfur source exhibit absorption at 688 nm and at 681 nm, respectively. Here, using DPE as a solvent, the absorption wavelength increases considerably compared to ODE as solvent. The reason may be due to the inadequate absorption of ODE owing to its structures.

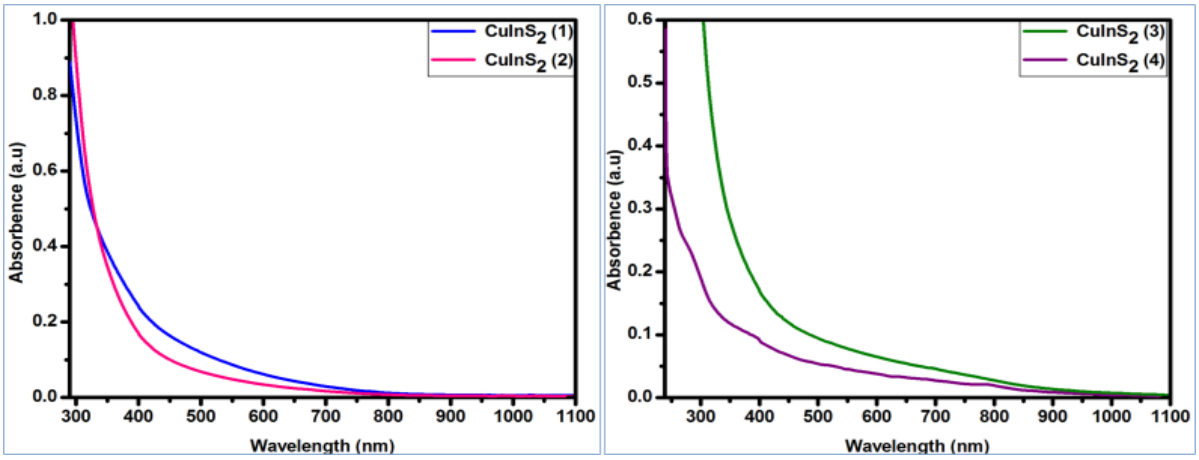

Figure 1. UV-Vis spectrum of $CuInS_2$ nanocrystals (1) ODE as solvent and sulfur powder as sulfur sources (2) ODE as solvent and DDT as sulfur sources (3) DPE as stabilizer and sulfur powder as sulfur sources (4) DPE as solvent and DDT as sulfur sources

B. Determination of Band Gap of $CuInS_2$ Nanocrystals

The onset absorption peak of the synthesized nanocrystals were determined by a least-squares fit of the linear region of a $(\alpha h\nu)^2$ vs. hν plot (A = absorbance, h = Planck's constant, and n = frequency), as presented in Figure. 2.

The calculated band gap energy by UV–vis results for the $CuInS_2$ nanocrystals synthesized by various solvents as well as sulfur source was about 1.90–2.20 eV, which showed a blue-shift in comparison to bulk $CuInS_2$ bulk(1.52 eV) due to the quantum confinement effects [25].

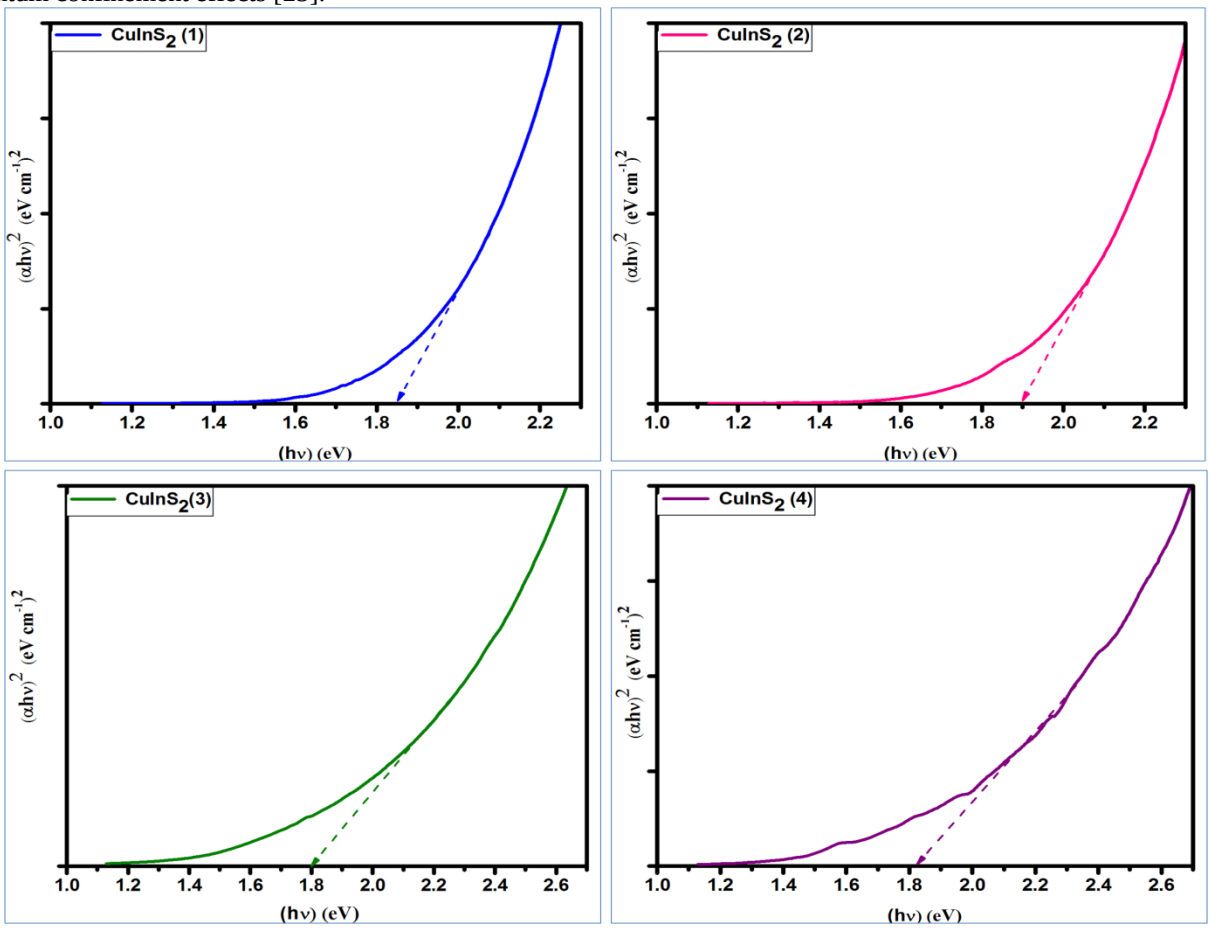

Figure 2. Bandgap of $CuInS_2$ nanocrystals (1) ODE as solvent and sulfur powder as sulfur sources (2) ODE as solvent and DDT as sulfur sources (3) DPE as stabilizer and sulfur powder as sulfur sources (4) DPE as solvent and DDT as sulfur sources

Table 1. The optical and electrochemical bandgap of $CuInS_2$ nanocrystals were determined by absorption spectra and cyclic voltammetry.

S.No	Samples	Band gap (eV)	
		Optical	Electrochemical
1	$CuInS_2$ (1)	1.84	1.84
2	$CuInS_2$ (2)	1.90	1.90
3	$CuInS_2$ (3)	1.80	1.80
4	$CuInS_2$ (4)	1.82	1.82

C. Determination of Band alignment using cyclic voltammetry

Cyclic voltammetry is an effective method to determine the band gaps and the energy levels (band alignment) of the HOMO and the LUMO of nanocrystals [26].

The oxidation process is related to the injection of a hole into the HOMO levels, and the reduction process is related to the injection of an electron into the LUMO levels.

The energy levels (E_g^{ec}) can be calculated from the onset oxidation potential (E_{ox}) and onset reduction potential (E_{red}), respectively, according to the following equations (1) and (2);

E_{HOMO} = -Ip = - (Eox+ 4.71) eV (1)

E_{LUMO} = -Ea = - (Ered + 4.71) eV (2)

The LUMO and HOMO energy levels and bandgap of the synthesized nanocrystals were obtained from cyclic voltammetric curves summarized in Table 2

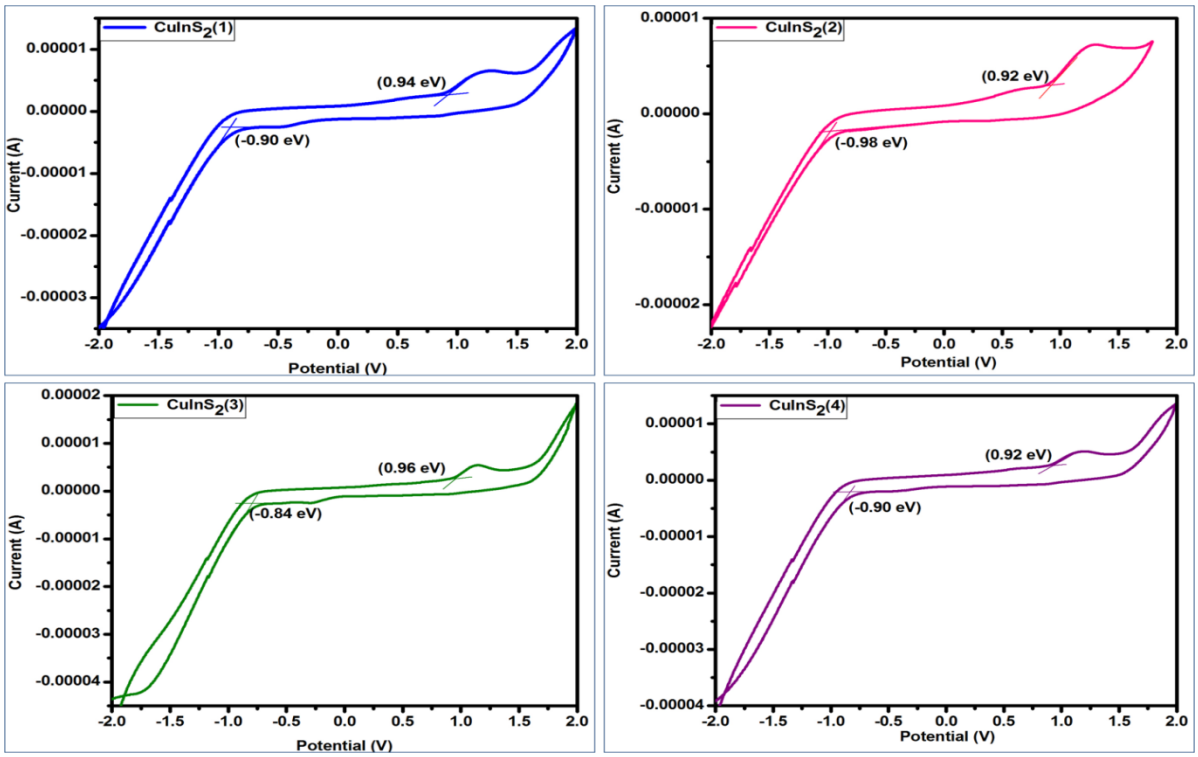

Figure 3. Cyclic voltammetry of OLA capped $CuInS_2$ nanocrystals. (1) ODE as solvent and sulfur powder as sulfur sources (2) ODE as solvent and DDT as sulfur sources (3) DPE as stabilizer and sulfur powder as sulfur sources (4) DPE as solvent and DDT as sulfur sources

Table 2. The band alignment and electrochemical bandgap (E_g^{ec}) of $CuInS_2$ nanocrystals were determined by cyclic voltammetric curves

S.No	Sample	Oxidation Potential (V)	HOMO (eV)	Reduction Potential (V)	LUMO (eV)	E_g^{ec} (eV)
1	$CuInS_2$ (1)	0.94	-5.65	-0.90	-3.81	1.84
2	$CuInS_2$ (2)	0.92	-5.63	-0.98	-3.73	1.90
3	$CuInS_2$ (3)	0.96	-5.67	-0.84	-3.87	1.80
4	$CuInS_2$ (4)	0.92	-5.63	-0.90	-3.81	1.82

D. Photoluminescence spectra

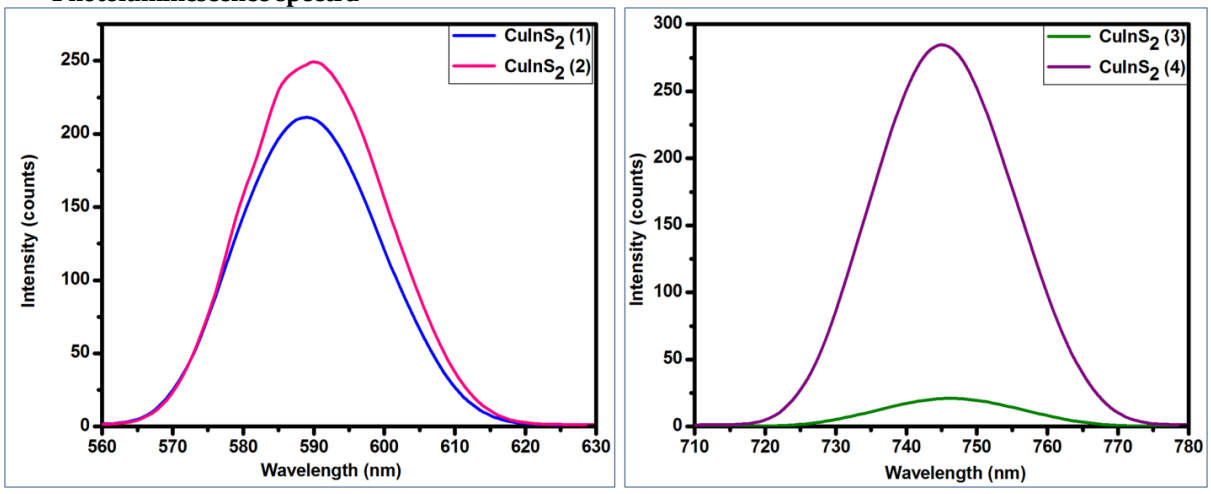

Figure 4. PL of OLA capped $CuInS_2$ nanocrystals. (1) ODE as solvent and sulfur powder as sulfur sources (2) ODE as solvent and DDT as sulfur sources (3) DPE as stabilizer and sulfur powder as sulfur sources (4) DPE as solvent and DDT as sulfur sources

Figure 4 shows the typical PL emission spectra of the OLA capped $CuInS_2$ nanoparticles prepared using different solvent and sulfur source. The PL spectra of $CuInS_2$ nanocrystals also exhibited shape and size dependent emissions. The

photoluminescence of the nanocrystals is complicated, because it is sensitive to surface structure, crystal sizes and shapes, chemical environment, and a number of interactions [27]. Figure.4 shows the evolution of PL emission spectra of $CuInS_2$ nanocrystals, which also exhibit shape-dependent emissions at 590 nm for zincblende $CuInS_2$ and 745 nm for wurtzite $CuInS_2$.

E. Crystal structure of $CuInS_2$ nanocrystals

Figure.5 reveals that the zinc blende and hexagonal $CuInS_2$ phase is formed by different solvent system like OLA/ODE and OLA/DPE combined with different sulfur source (sulfur powder or DDT).

Figure.5a shows the diffraction peaks exists cubic zinc-blende structure using ODE as solvent. The diffraction peak of 2θ value falls at 27.85 to 27.91 and second 2θ value lies between 46.29 and 46.43 as in the reported value[29]. The four assigned planes are (111), (200), (204), (311) and it shows zinc blende structure. It means that the structure is zinc blende with space groups 142d (112) (JCPDS Card No: 85-1575). The lattice parameters of the synthesized $CuInS_2$ are a =5.50Å and they match with literature values [28]. The formation of four main peaks proves that the existence of formation of zincblende $CuInS_2$. No other diffraction peaks can be detected, which indicates that the obtained samples are pure zinc blended $CuInS_2$ without any binary sulphides of Cu_2S, CuS, or In_2S_3.

Figure.5b shows that the structure is similar to the wurtzite structure with the Cu and In atoms randomly distributed on the cation sites and the lattice parameters were refined to c = 6.478 Å and a = 3.944 Å, respectively [28].

The grain size of the synthesized $CuInS_2$ nanocrystals can be determined from XRD using the Debye-Scherrer equation (3),

$$D = \frac{0.9\lambda}{\beta \cos\theta} \qquad (3)$$

where λ is the wavelength λ = 1. 5418 Å, β is the full width at half maximum (FWHM) and θ is the angle of strong peak. The average size of the synthesized OLA capped $CuInS_2$ nanocrystals are between 10 and 15 nm, respectively.

The lattice parameter values for cubic and hexagonal structure of $CuInS_2$ nanocrystals are calculated from the following equations (4) and (5);

Cubic : $$\frac{1}{d^2} = \frac{h^2+hk+k^2}{a^2} \qquad (4)$$

Hexagonal : $$\frac{1}{d^2} = \frac{4}{3}\left(\frac{h^2+hk+k^2}{a^2}\right) + \frac{l^2}{c^2} \qquad (5)$$

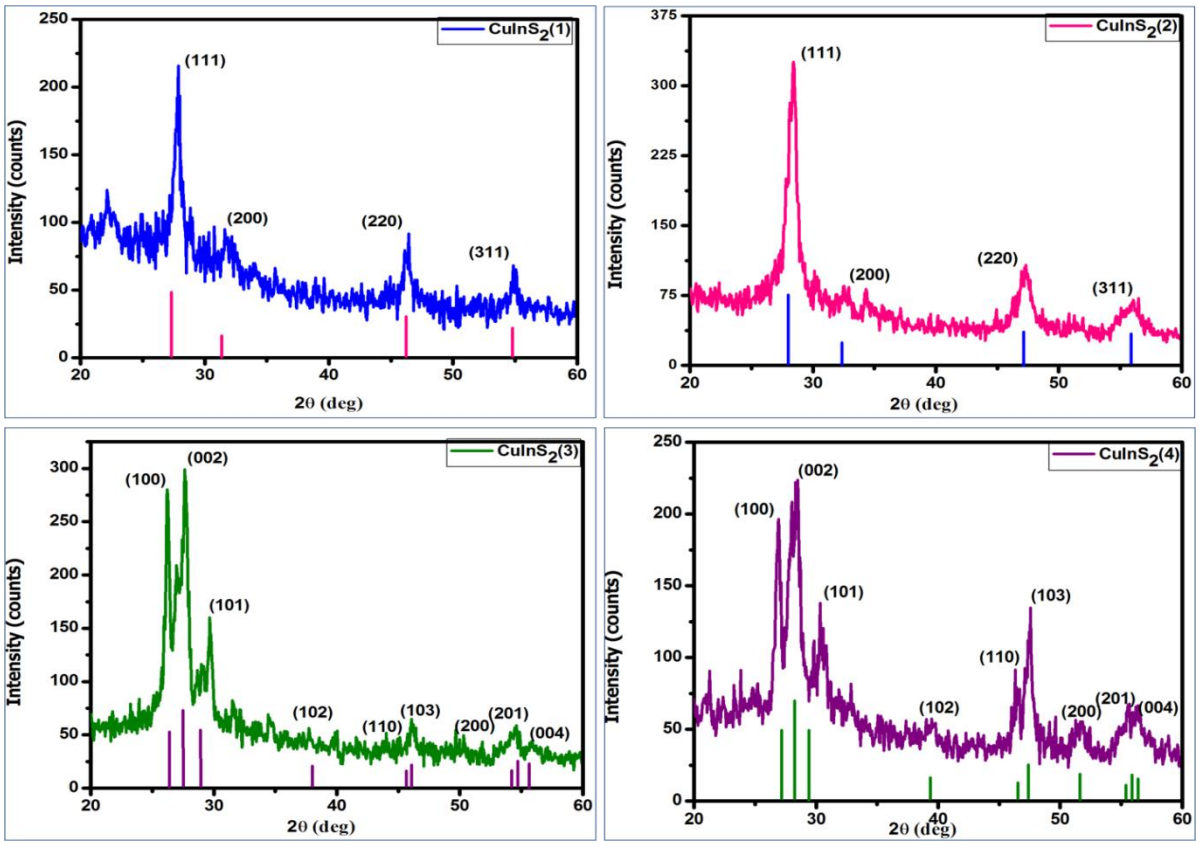

Figure 5. XRD patterns of OLA capped $CuInS_2$ nanocrystals. (1) ODE as solvent and sulfur powder as sulfur sources (2) ODE as solvent and DDT as sulfur sources (3) DPE as stabilizer and sulfur powder as sulfur sources (4) DPE as solvent and DDT as sulfur sources

F. Morphological structure of $CuInS_2$ Nanocrystals

Figure.6 shows the effect of solvents and sulfur source on morphology of OLA capped $CuInS_2$ nanocrystals by TEM. The $CuInS_2$ nanocrystals shows nearly spherical morphology when ODE as a non-coordinating solvent whereas hexagonal-like nanoplates were obtained when DPE was used as a coordinating solvent.

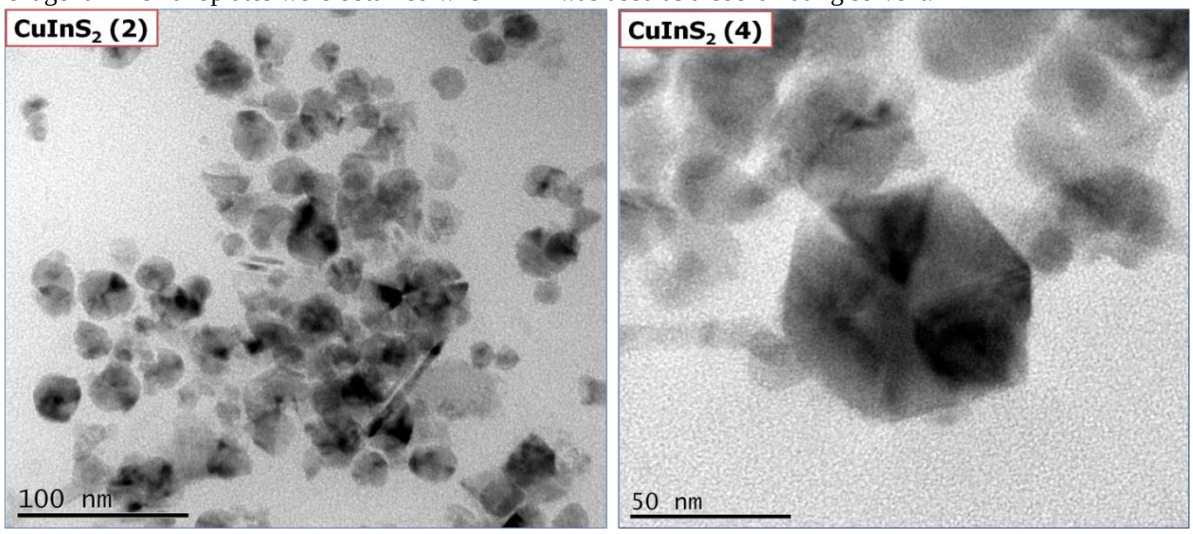

Figure 6. TEM images of OLA capped $CuInS_2$ nanocrystals. (2) ODE as solvent and DDT as sulfur sources (4) DPE as solvent and DDT as sulfur sources.

G. Elemental compositions of $CuInS_2$ nanocrystals

Energy dispersive x-ray spectroscopy (EDX) was further used to determine the composition ratios of the $CuInS_2$ (2) and $CuInS_2$ (4) nanocrystals are shown in Fig.7. The EDX spectrum revealed that the synthesized nanocrystals are nearly stoichiometric in nature.

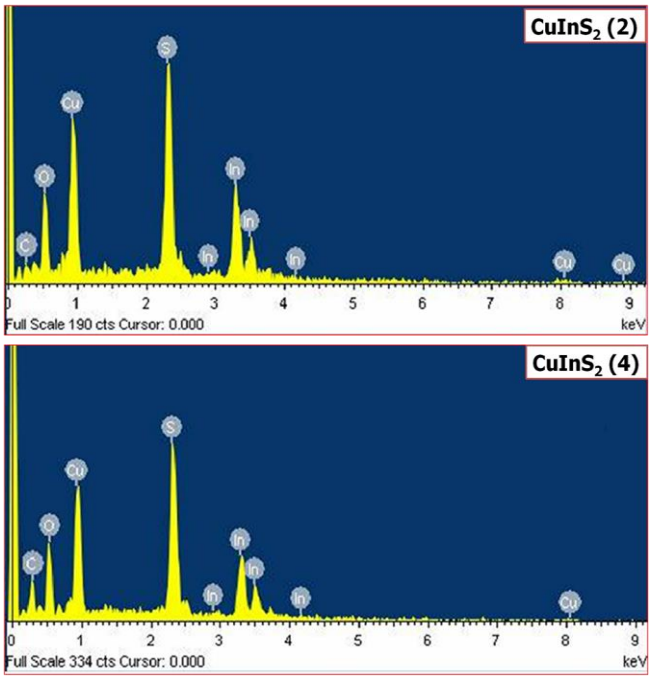

Figure 7. EDX images of OLA capped $CuInS_2$ nanocrystals 2) ODE as solvent and DDT as sulfur sources (4) DPE as solvent and DDT as sulfur sources.

IV. CONCLUSION

In summary, OLA-Capped $CuInS_2$ nanocrystals were synthesized by hot injection method. The morphology, optical properties and size of the $CuInS_2$ nanocrystals were tuned by changing the solvent (coordinating and non-coordinating) and sulfur source (sulfur powder and DDT). The PL emission spectra of the as-prepared $CuInS_2$ nanocrystals exhibit at 590 nm for ZB-$CuInS_2$ and at 745 nm for WZ-$CuInS_2$ nanocrystals. XRD and TEM analyses confirmed that the nanocrystals possessed pure zinc blende and wurtzite phase for OLA/ODE/S and OLA/DPE/S based $CuInS_2$ nanocrystals. TEM images showed that the synthesized nanocrystals (2) and (4) are spherical and hexagonal-like morphology.

REFERENCES

[1]. Connor S.T, Hsu C.M, Weil B.D, Aloni S, Cui Y., *J Am Chem Soc.*, 131,4962–4966 (2009).
[2]. Yu Y.X, Ouyang W.X, Liao Z.T, Du B.B, Zhang W.D., *ACS Appl. Mater. Interfaces*,6, 8467–74 (2014).
[3]. Norako M.E, Franzman M.A, Brutchey R.L., *Chem. Mater.*, 21, 4299–4304 (2009).
[4]. Valde´s M.H, Berruet M, Goossens A, Va´zquez M., *Surf. Coat. Tech.*, 204, 3995 4000 (2010).
[5]. Aboulaich A, Michalska M, Schneider R, Potdevin A, Deschamps J, Deloncle R, Chadeyron G, Mahiou R., *ACS Appl. Mater. Interfaces.*, 6, 252–258 (2014)
[6]. Tomic S, Bernasconi L, Searle B.G, Harrison N.M., *J. Phys. Chem. C.*, 118, 14478–14484 (2014).
[7]. Yong K.T, Roy I, Hu R, Ding H, Cai H., Zhu J, Zhang X, Bergeya E.J, Prasad P.N., *Integr. Biol.*, 2, 121–129 (2010).
[8]. Chen Y, Li S, Huang L, Pan D., *Inorg. Chem.*, 52, 7819–7821 (2013).
[9]. Yoon H, Na S.H, Choi J.Y, Kim M.W, Kim H, An H.S, Min B.K, Ahn S.J, Yun J.H, Gwak J, Yoon K.H, Kolekar S.S, Hest M.F.A.M.V, Al-Deyab S.S, Swihart M.T, Yoon S.S., *ACS Appl. Mater. Interfaces.*, 6, 8369–8377 (2014)
[10]. Aldakov D, Lefrancois A, Reiss P., *J. Mater. Chem. C.*, 1, 3756–3776 (2013)
[11]. Binsma J.J.M, Giling L.J, Bloem J., *J. Cryst. Growth.*, 50, 429 (1980).
[12]. Lu X.T, Zhuang Z.B, Peng Q, Li Y.D., *Cryst. Eng. Comm.*, 13, 4039–4045(2011).
[13]. Gusain M, Kumar P, Nagarajan R., *RSC Advances.*, 3, 18863–18871 (2013).
[14]. Zhong H, Li Y, Ye M, Shu Z, Shou Y, Yang C and Li Y., *Nanotechnology.*,18,025602 (2007).
[15]. Nose K, Omata T and Otsuka-Yao-Matsuo S., *J. Phys.Chem. C.*,113,3455 (2009)
[16]. GuO Q, Kim S J, Kar M, Shafarman W.N, Birkmire R.W, Stach E.A, Agrawal R and Hillhouse H.W., *Nano Lett.*,8,2982 (2008)
[17]. Norako M. E, Brutchey R.L, *Chem. Mater.*,22,1613 (2010).
[18]. Castro S.L, Bailey S.G, Raffaelle R.P, Banger K.K and Hepp A.F, *Chem. Mater.*,15,3142 (2003).
[19]. Wu C.C, Shiau C.Y, Ayele D.W, Cheng M.Y, Chiu C.Y, Hwang B.J, *Chem. Mater.*,22,4185 (2010).
[20]. Koo B, Patel R.N, Korgel B.A, *J. Am. Chem. Soc.*,131,3134 (2009).
[21]. Li B, Xie Y, Huang J, Qian Y., *Adv. Mater.*,11, 1456 (1999).
[22]. Jiang Y, Wu Y, Mo X, Yu W, Xie Y and Qian Y., *Inorg.Chem.*,39, 2964 (2000).
[23]. Malik M. A, O' Brien P and Revaprasadu N., *Adv. Mater.*,11,1441 (1999).
[24]. Kruszynska M, Borchert H, Parisi J, Kolny-Olesiak J, *J Nanopart Res1*3, 5815–5824(2011)
[25]. M. Yousefi, M. Sabet, M. Salavati-Niasari, S.M. Hosseinpour-Mashkani, *J. Clus. Sci.* 23 (2012) 491.
[26]. H.Z. Zhong, S.S. Lo, T. Mirkovic, Y.C. Li, Y.Q. Ding, Y.F. Li, G.D. Scholes, *ACS Nano* 4 (2010) 5253–5262.
[27]. Y.C. Li, X.H. Li, C.H. Yang, Y.F. Li, *J. Mater. Chem.* 13 (2003) 2641.Huang W. C, Tseng C. H, Chang S. H, Tuan H.Y, Chiang C. C, Lyu L. M, Huang M. H; *Langmuir.* 28 (2012), 8496−8501.